Influence of hydrogen on electrochemical behavior of Ni-based superalloy 718

Grégory Odemer, Eric Andrieu, Christine Blanc

Short Communication

Influence of hydrogen on electrochemical behavior of Ni-based superalloy 718

Grégory Odemer[*], *Eric Andrieu*, *Christine Blanc*

CIRIMAT, Université de Toulouse, CNRS, INPT, UPS, ENSIACET, 4 Allée Emile Monso, BP 44362, 31030 Toulouse Cedex 4, France

ARTICLE INFO

Keywords:
Nickel alloys
Hydrogen embrittlement
Electrochemistry
Galvanic coupling

ABSTRACT

Numerous studies have shown that Ni-based superalloy 718 may be sensitive to hydrogen embrittlement and have highlighted the dominant roles played by the hydrogen solubility and the hydrogen trapping. Samples were hydrogenated by cathodic polarization in molten salts under different conditions to vary the diffusible hydrogen content and to saturate the different hydrogen traps present in the microstructure strengthened by precipitation. Open circuit potential and galvanic coupling measurements were conducted in order to characterize the effect of diffusible and trapped hydrogen on electrochemical behavior and to discuss the possibility of galvanic coupling between zones with different hydrogen contents.

Introduction

Alloy 718 is a Ni-based superalloy that is widely used for high-temperature applications, particularly for structural components in the aeronautic and nuclear industries, due to its good mechanical properties. This alloy is strengthened both by structural hardening and by solid solution hardening [1]. The typical strengthening heat treatment applied to alloy 718 consists of a dwell of 8 h at 720 °C, followed by cooling at 50 °C/h and a final dwell of 8 h at 620 °C. This process leads to the precipitation of γ″ (metastable and coherent with the matrix, tetragonal $D0_{22}$ structure, Ni_3Nb composition, disc-shaped (20 nm diameter × 10 nm thickness)) and γ′ (stable and coherent with the matrix, cubic $L1_2$ structure, $(Al,Ti)Ni_3$ composition, spherical shape (20 nm)) phases embedded in a γ matrix (volume fraction of γ′−γ″ = 16% and γ′/γ″ ratio = 1/4). Some primary carbides precipitates are also present in the microstructure [2].

Under operating conditions, despite a good resistance to stress corrosion cracking (SCC), corrosion processes may induce local hydrogen enrichment at the material surface and/or in the vicinity of localized corrosion defects. Consequently, a hydrogen-assisted SCC phenomenon can occur under complex stress and strain states [3]. The hydrogen embrittlement (HE) of Ni-based alloys is generally exacerbated when the alloys are submitted to mechanical loading, suggesting that hydrogen diffusion occurs along stress gradients as well as hydrogen transport by dislocations during plastic deformation [4–14]. Hydrogen transport by mobile dislocations can lead to local hydrogen enrichment in the dislocation pile-ups close to precipitates/interfaces, which favors crack initiation. Galliano

* *Corresponding author.*
E-mail address: gregory.odemer@ensiacet.fr (G. Odemer).
https://doi.org/10.1016/j.ijhydene.2017.11.081

et al. have confirmed this point and have shown a strong susceptibility of the strengthened alloy 718 to HE after cathodic hydrogen charging [2].

Effect of hydrogen on rupture modes

In this work, samples were hydrogenated by cathodic charging in molten salts at 150 °C as done by Galliano et al. [2]. All the characteristics of these chargings are detailed in this previous work as well as hydrogen content measurements using a Galileo Bruker analyzer and the procedure of hydrogen desorption tests [2]. The fracture surfaces obtained after tensile tests performed at 25 °C and $\dot{\varepsilon} = 10^{-3}\ s^{-1}$ for pre-hydrogenated samples of strengthened alloy 718 are presented in Fig. 1 and showed both transgranular (cleavage) (Fig. 1a and b) and intergranular brittle fracture (Fig. 1c).

Two main HE mechanisms in relation to the hydrogen-trapping mechanism are generally considered to explain the fracture surfaces: the hydrogen-enhanced localized plasticity (HELP) and hydrogen-induced decohesion (HID) mechanisms [15]. The HELP mechanism corresponds to an increase in dislocation mobility by the reduction of the elastic interactions between obstacles and perfect and partial dislocations [16]. Associated with a hydrogen transport phenomenon facilitated by dislocations, this mechanism leads to local segregation of hydrogen on {111} planes, inducing cleavage, as well as the decohesion of particles/matrix interfaces (HID mechanism) [17,18].

Intergranular brittle fracture suggested that hydrogen preferentially diffused/segregated along grain boundaries, partly due to the hydrogen-trapping mechanism on carbides that reduced the cohesive strength of the grain boundaries structure. But, the low density of intergranular carbides suggested rather that the grain boundaries chemistry and crystallographic relations could have a strong effect on intergranular rupture too as well as the possibility of intergranular element segregations such as Nb or P [19–21].

Study of hydrogen trapping reversibility

So these results have shown the strong influence of hydrogen traps on HE susceptibility of the alloy 718 and particularly on the rupture modes. For a better understanding of the hydrogen desorption phenomena in relation with hydrogen trapping, desorption heat treatments were conducted at two temperatures, i.e. 25 °C and 320 °C, during 300 min for samples all pre-hydrogenated in molten salts at 150 °C for 8 h. To compare the evolution of the hydrogen content between each desorption temperature, the hydrogen content was measured relative to the initial hydrogen content [H_0] measured for a pre-hydrogenated sample immediately after charging. All hydrogen contents were measured using a Galileo Bruker analyzer [2]. The results of this analysis are given in Fig. 2.

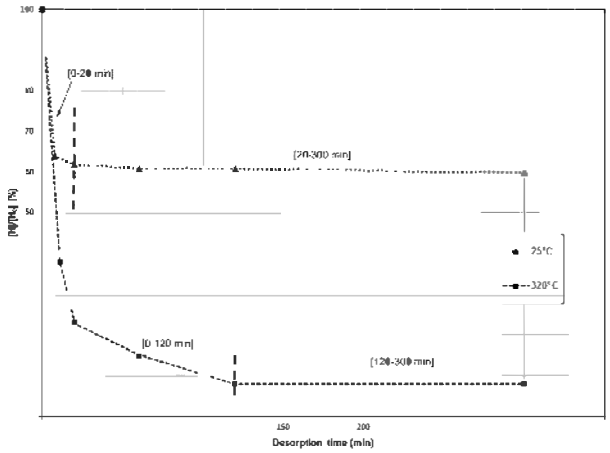

Fig. 2 – Evolution of hydrogen content in 8 h H-charged alloy 718 during 300 min at 25 °C and 320 °C.

For both temperatures, two successive regimes were characterized. A preliminary step characterized by a strong hydrogen desorption followed by a second step corresponding to a stagnation of the hydrogen content:

- Hydrogen desorption regime: [0–20 min] at 25 °C and [0–120 min] at 320 °C.

The hydrogen desorption was relatively rapid, and the level of desorption was dependent on the temperature. Considering that the main hydrogen traps characteristic of the strengthened alloy, i.e. carbides and strengthening precipitates/matrix interfaces, are irreversible [5,22], the rapid and strong hydrogen content decrease observed in the desorption curves

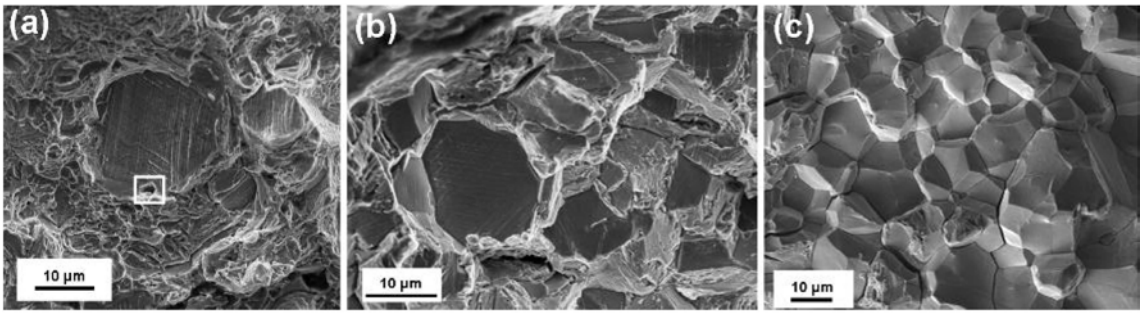

Fig. 1 – Fracture surfaces observations of pre-hydrogenated samples of strengthened alloy 718 after tensile test. Transgranular rupture (cleavage) related to hydrogen trapping (a) on carbide/matrix interfaces and (b) on strengthening precipitates/matrix interfaces and (c) intergranular rupture related to hydrogen diffusion/segregation along grain boundaries.

was related partially to the desorption of interstitial hydrogen, i.e. bulk diffusivity, and to a large extent to the hydrogen diffusion by grain boundaries, which have been characterized as short-circuit paths of diffusion in several studies [12–14,23]. Indeed Harris and Latanision have shown that the values of hydrogen diffusion coefficient in grain boundaries could be 40 to 1000 larger than the lattice diffusion coefficient at 30 °C for nickel with very small grain size (0.1 μm) [23]. In this work, the grain size of the alloy 718 was around 9 μm that remains small and could induce a significant difference between grain boundary and lattice diffusion coefficients. However, this does not exclude that hydrogen desorption could be partially related to the bulk diffusivity. Moreover, this fast and significant hydrogen desorption could be enhanced also by the fact that cathodic charging led to a strongly H-enriched zone under the surface exposed to the molten salts and finally to a high apparent solubility in hydrogen [2], higher than data usually found in literature [24].

- Hydrogen content stagnation regime: [20–300 min] at 25 °C and [120–300 min] at 320 °C.

The different dwells observed for each temperature correspond to the hydrogen still present in the lattice and in grain boundaries and to the hydrogen trapped irreversibly on γ′–γ″ precipitates/matrix interfaces and carbides. These results regarding hydrogen desorption clearly suggested that precipitates/matrix interfaces were saturated in hydrogen after hydrogen cathodic charging, given that hydrogen desorption is mainly due to the partial desorption of interstitial hydrogen and mainly to the hydrogen desorption by grain boundaries. Finally, after 300 min of desorption, samples heat treated at 320 °C presented a hydrogen content around 10 ppmw, i.e. 6 times lower than samples desorbed at 25 °C (hydrogen content around 60 ppmw). This difference could be explained by the increase of the hydrogen diffusion coefficients with temperature (both grain boundary and lattice diffusion coefficients) and by the fact that hydrogen trapped in grain boundaries in relation with intergranular segregations such as Nb or P could egress at 320 °C.

Effect of hydrogen on electrochemical behavior

In a previous work, it was shown that hydrogen was able to modify the electrochemical behavior of different metallic alloys, and particularly their open circuit potential (OCP) [25] but also their local surface potential, measured by means of Kelvin probe force microscopy [26–28]. Moreover, recently rigorous calibrations of the KFM technique confirmed the correlation between the corrosion potential and the inverted KFM potential measured by a scanning Kelvin probe (SKP) in 80% relative humidity [29] and the relation, for dry surfaces, between the amount of available hydrogen with the work function which can be considered as an electrode potential [30].

Several works of Pound et al. have highlighted the role of hydrogen on electrochemical behavior of Ni-based alloys, in relation with diffusion and trapping phenomena. So they used a potentiostatic double-step technique to study hydrogen atom ingress into a planar test electrode of the studied alloy. The technique involves generating hydrogen atoms at a constant cathodic potential, then stepping the potential to a more positive value and recording the anodic current and charge associated with the removal of hydrogen atoms from the electrode [31].

On the basis of all these results, the effect of hydrogen on OCP of alloy 718 was investigated by measuring the OCP vs. immersion time at 25 °C in 0.5 M NaCl medium for pre-hydrogenated samples for different cathodic charging times, i.e. 0.5 h, 1 h, 8 h and 16 h and for a sample pre-hydrogenated during 8 h and then heat treated during 300 min at 320 °C before electrochemical characterization. The results of these measurements are given in Fig. 3.

The evolution of OCP vs. immersion time is given for comparison for a H-free sample (Fig. 3) and highlighted that OCP after 450 min, i.e. 0.09 V/SCE, was not stabilized. A longer test duration was required, i.e. around 1000 min as shown in Fig. 4 in order to reach an OCP stabilization in relation with a slow passivation of the material surface and with the low aggressivity of the medium for this type of Ni-based superalloy. The measurements on H-charged samples allowed to confirm the effect of hydrogen on OCP values. It was shown that hydrogen shifted the OCP values towards more negative potentials in relation with the cathodic charging time and therefore with the hydrogen content in subsurface and that hydrogen stabilized quickly the OCP. Such a result raised the question of how hydrogen could affect the OCP. It is true that changes in OCP would be indicative of changes in the surface. For example, as suggested by Protopopoff et al. [32], the adsorption of hydrogen on the metallic surface should lead to a change in OCP. However, the relationship between the amplitude of the changes in OCP and the cathodic charging time suggested that the influence of hydrogen on OCP was more complex. As suggested in the literature, by modifying the electronic output work [26–30], the hydrogen should affect the Volta Potential as well as the OCP measured in solution. Although no clear mechanism explaining the role of hydrogen on the electronic output work was established, it was assumed that hydrogen distorts the metallic lattice leading to the variations observed. It could be assumed that the influence of hydrogen on OCP should depend on the precipitation state of the material. Indeed, the precipitates which act as trapping sites distort the lattice and/or create interfaces at which the hydrogen atoms will distort the lattice less. In this sense, the influence of hydrogen on OCP should give indication about the interaction between hydrogen and precipitates/matrix interfaces in subsurface as recently shown by Oger et al. [33]. Further, analysis of the OCP curves requires to consider H desorption during OCP measurements at 25 °C, as shown in Fig. 2. According to the results of desorption treatments (Fig. 2), after 20 min at 25 °C, for a sample hydrogenated for 8 h, the hydrogen content was stabilized with only strongly trapped hydrogen present inside the material. Since OCP curves for 1, 8 and 16 h of charging are similar (Fig. 3), it was possible to confirm that a cathodic charging of 1 h was sufficient to saturate precipitates/matrix interfaces in subsurface. However, for a 0.5 h duration, the interfaces seemed to be only partially saturated that explained the less negative OCP values measured. Then, the evolution of OCP values at the beginning

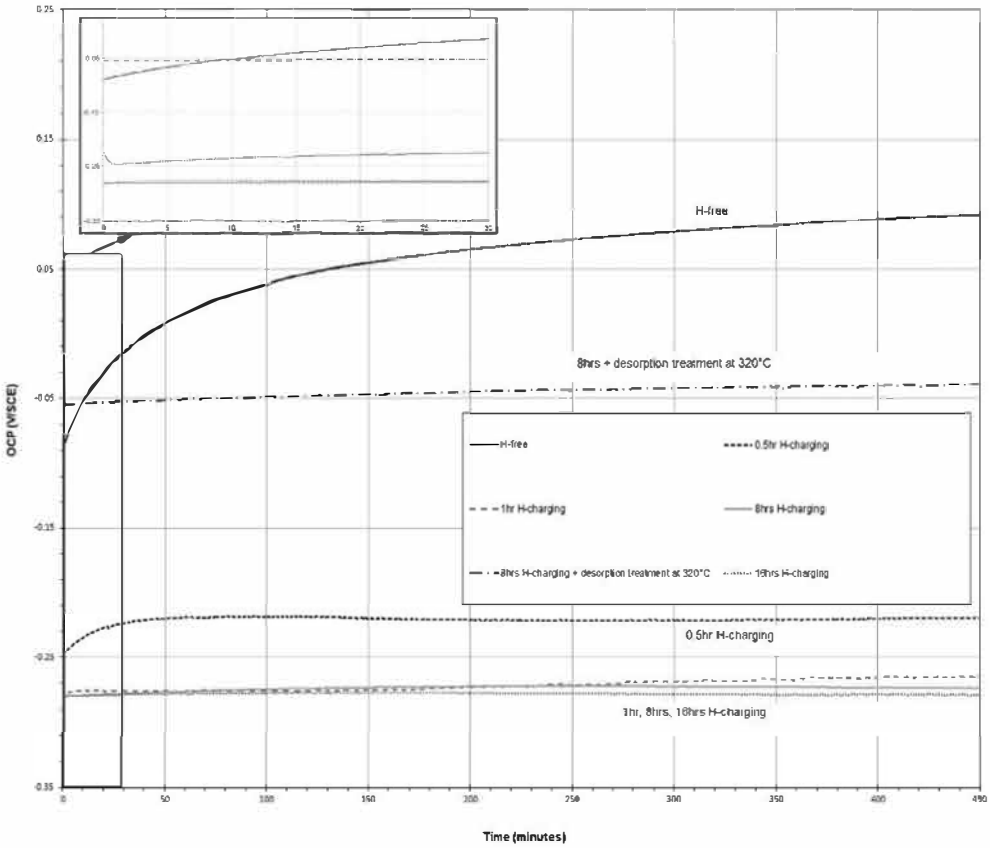

Fig. 3 – OCP (V/SCE) vs. time (minutes) of H-free, pre-hydrogenated (0.5 h, 1 h, 8 h and 16 h) and pre-hydrogenated + heat-treated at 320 °C samples.

of the electrochemical test performed on 8 h H-charged sample could be related to the strong hydrogen desorption at 25 °C during the first minutes of desorption test: the time required for OCP stabilization was in the same order of magnitude than diffusible hydrogen desorption time, i.e. 20–30 min, observed in Fig. 2. The most important desorption range for 0.5 h H-charged sample could be explained by the fact that OCP value was more susceptible to hydrogen desorption given that precipitates/matrix interfaces were not saturated for this duration of cathodic charging. It was also observed that the OCP value of the sample pre-hydrogenated during 8 h and heat treated during 300 min was intercalated between the OCP values of a H-free sample and pre-hydrogenated samples. According to the desorption tests (Fig. 2), the heat treatment performed at 320 °C led to the desorption of interstitial hydrogen and mainly of hydrogen trapped in grain boundaries in a larger extent than for hydrogen desorption occurring during OCP measurements at 25 °C which explained the less negative OCP values observed. The role of diffusible hydrogen on OCP has already been observed by Shaller and Scully [28] and diffusible hydrogen undoubtedly contributes to explain the OCP values. But, the difference in OCP values between a H-free sample and a outgassed sample was probably related to the hydrogen still trapped at matrix/precipitates interfaces given it was assumed that diffusible hydrogen content was negligible after the heat desorption treatment according to the diffusion calculations and the hydrogen content measurements and tensile surface factures. Indeed hydrogen content for H-free, H-charged and outgassed sample was respectively 0.5, 58 and 5.2 ppmw. Mechanical tests performed on H-free and H-charged tensile samples showed that hydrogen in grain boundaries induced intergranular rupture and hydrogen trapped at carbides and matrix/precipitates interfaces induced cleavage [2]. The fracture surface of the outgassed sample has shown only cleavage that reinforced the fact that hydrogen content after desorption treatment was mainly related to hydrogen trapped at matrix/precipitates interfaces

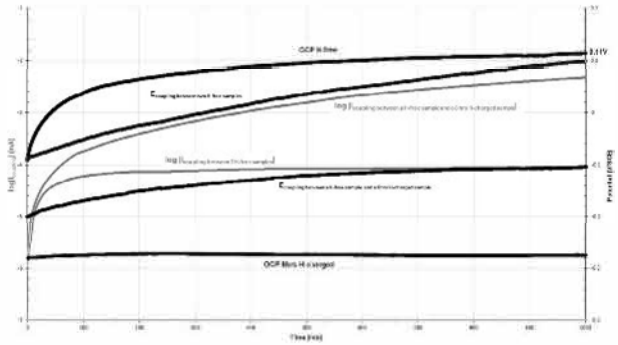

Fig. 4 – Galvanic coupling tests for two H-free electrodes and a H-free electrode coupled with a hydrogen pre-charged electrode.

and thus responsible for a large part for the OCP value according to the work of Oger et al. [33].

These results have shown that hydrogen was able to modify the electrochemical behavior of alloy 718 in relation with diffusible and trapped hydrogen content. So it could be considered that, for a hydrogenated material presenting a heterogeneous microstructure, the local hydrogen content could strongly vary, so that local galvanic coupling between zones with different hydrogen concentrations could occur. To confirm this hypothesis, a galvanic coupling test was performed in 0.5 M NaCl at 25 °C between a sample pre-charged in hydrogen during 8 h and a H-free sample. A preliminary test was performed with two H-free samples as reference. The results are presented in Fig. 4.

At first, the coupling tests performed with two H-free samples showed that the common potential measured was logically close to the value of the OCP of a H-free sample, i.e. 0.11 V/SCE after 1000 min. Moreover, these tests allowed to determine the reference coupling current, i.e. 10^{-4} mA after stabilization. The fact that this coupling current has a non-zero value could be explained by the residual hydrogen content of H-free material, i.e. between 0.2 and 0.5 ppmw depending on the samples that could induce a slight coupling [2]. The common potential measured during coupling test between a H-free sample and a 8 h H-charged sample, i.e. −0.1 V/SCE, was logically comprised between OCPs of H-free sample and 8 h H-charged sample, and corresponded to an anodic polarization for the 8 h H-charged sample. This result showed that the H-charged sample was the sacrificial anode during the coupling test. This result was confirmed by the galvanic coupling current measured, i.e. around 2 orders of magnitude higher than the current obtained during coupling of the two H-free samples. Moreover the increase of the difference between the coupling currents as the function of time suggested that the galvanic coupling due to hydrogen led to a self-catalyzed mechanism.

Conclusion

Therefore, it was demonstrated that H enrichment led to a shift of the OCP of alloy 718 towards more negative values. This result is particularly important because it suggests that in a complex microstructure with a heterogeneous hydrogen distribution, local galvanic couplings could be active in parallel to classical SCC and HE phenomena, enhancing the resultant damage. Further local electrochemical analysis such as KFM will be performed to support these first conclusions.

REFERENCES

[1] Oblak JM, Paulonis DF, Duvall DS. Coherency strengthening in Ni base alloys hardened by DO_{22} γ″ precipitates. Metall Trans 1974;5:143–53.

[2] Galliano F, Andrieu E, Blanc C, Cloué JM, Connetable D, Odemer G. Effect of trapping and temperature on the hydrogen embrittlement susceptibility of alloy 718. Mat Sci Eng A 2014;611:370–82.

[3] Totsuka N, Lunarska E, Cragnolino G, Szklarska-Smialowska Z. Effect of hydrogen on the intergranular stress corrosion cracking of alloy 600 in high temperature aqueous environments. Corrosion 1987;43:505–14.

[4] Lecoester F, Chene J, Noel D. Hydrogen embrittlement of the Ni-base Alloy 600 correlated with hydrogen transport by dislocations. Mater Sci Eng A 1999;262:173–83.

[5] Chene J, Brass AM. Role of temperature and strain rate on the hydrogen-induced intergranular rupture in alloy 600. Metall Trans A 2004;35:457–64.

[6] Symons DM. The effect of hydrogen on the fracture toughness of alloy X-750 at elevated temperatures. J Nucl Mater 1999;265:225–31.

[7] Hicks PD, Altstetter CJ. Internal hydrogen effects on tensile properties of iron- and Ni-Base superalloys. Metall Trans A 1990;21:365–72.

[8] Fournier L, Delafosse D, Magnin T. Cathodic hydrogen embrittlement in alloy 718. Mater Sci Eng A 1999;269:111–9.

[9] Hicks PD, Altstetter CJ. Hydrogen-enhanced cracking of superalloys. Metall Trans A 1992;23:237–49.

[10] Fukuyama S, Yokogawa K. Effect of heat treatments on hydrogen environment embrittlement of alloy 718. In: Superalloys 718, 625, 706 and various derivatives, Pittsburgh; 1994. p. 807–16.

[11] Wei W. The effect of hydrogen on the high temperature mechanical properties of IN 718. In: Superalloys 718, 625, 706 and various derivatives, Pittsburgh; 1997. p. 705–14.

[12] Liu L, Zhai C, Lu C, Ding W, Hirose A, Kobayashi KF. Study of the effect of δ phase on hydrogen embrittlement of Inconel 718 by notch tensile tests. Corr Sci 2005;47:355–67.

[13] Sjoberg G, Cornu D. Hydrogen embrittlement of cast alloy 718 effects of homogeneization, grains size and δ-phase. In: Superalloys 718, 625, 706 and various derivatives, Pittsburgh; 2001. p. 679–90.

[14] Liu L, Tanaka K, Hirose A, Kobayashi KF. Effects of precipitation phases on the hydrogen embrittlement sensitivity of Inconel 718. Sci Tech Adv Mater 2002;3:335–44.

[15] Birnbaum HK, Robertson IM, Sofronis P, Teter D. Mechanisms of hydrogen related fracture – a review. In: Magnin T, editor. Proceeding of the second international conference on corrosion-deformation interactions. Nice, France: The Institute of Materials; 1996. p.172–195.

[16] Ferreira PJ, Robertson IM, Birnbaum HK. Hydrogen effects on the interaction between dislocations. Acta Mater 1998;46:1749–57.

[17] Moody NR, Perra MW, Robinson SL. Hydrogen-induced cracking in an iron-based superalloy. In: Moody NR, Thompson AW, editors. Hydrogen effects in material behavior; 1990. p. 625–34.

[18] Robinson SL, Somerday BP, Moody NR. Hydrogen embrittlement of stainless steel. In: Proceedings of the 11th international conference on fracture, Turin, Italy; 2005. p. 672.

[19] Was GS. Grain-boundary chemistry and intergranular fracture in austenitic nickel-base alloys – a review. Corrosion 1990;46:319–30.

[20] Yonezawa T, Onimura K, Sakamoto O, Sasaguri N, Nakata H, Susukida H. Effect of heat treatment on stress corrosion cracking resistance of high-nickel alloys. In high-temperature water. In: Proceedings of the international symposium on environmental degradation of materials in nuclear power systems water reactors. Houston, TX: NACE; 1984. p. 345–66.

[21] Miglin MT, Domain HA. Microstructure and stress corrosion resistance of alloy X750, 718 and A-286 in light water reactor environments. In: Scarberry RC, editor. Corrosion of nickel-base alloys. Materials Park, OH: ASM Int; 1985. p. 147–64.

[22] Young GA, Scully JR. Evidence that carbide precipitation produces hydrogen traps in Ni-17Cr-8Fe alloys. Scr Mater 1997;36:713–9.
[23] Harris TM, Latanision RM. Grain boundary diffusion of hydrogen in Nickel. Metall Trans 1991;22A:351–5.
[24] Robertson WM. Hydrogen permeation and diffusion in Inconel 718 and Incoloy 903. Metall Trans 1977;A8:1709–12.
[25] Giffard K. Study of the sealing mechanisms of the anodic films on aeronautical 2024 aluminium alloy [Thesis of the Université de Toulouse]. 2015.
[26] Larignon C, Alexis J, Andrieu E, Lacroix L, Odemer G, Blanc C. Investigation of Kelvin probe force microscopy efficiency for the detection of hydrogen ingress by cathodic charging in an aluminium alloy. Scr Mater 2013;68:479–82.
[27] Larignon C, Alexis J, Andrieu E, Lacroix L, Odemer G, Blanc C. Combined Kelvin probe force microscopy and secondary ion mass spectrometry for hydrogen detection in corroded 2024 aluminium alloy. Electrochim Acta 2013;110:484–90.
[28] Schaller RF, Scully JR. Spatial determination of diffusible hydrogen concentrations proximate to pits in a Fe–Cr–Ni–Mo steel using the scanning Kelvin probe. Electrochem Commun 2016;63:5–9.
[29] Cook AB, Barrett Z, Lyon SB, McMurray HN, Walton J, Williams G. Calibration of the scanning Kelvin probe force microscope under controlled environmental conditions. Electrochim Acta 2012;66:100–5.
[30] Senöz C, Evers S, Stratmann M, Rohwerder M. Scanning Kelvin Probe as a highly sensitive tool for detecting hydrogen permeation with high local resolution. Electrochem Commun 2011;13:1542–5.
[31] Pound BG. Hydrogen trapping in precipitation-hardened alloys. Acta Metall Mater 1990;38:2373–81.
[32] Protopopoff E, Marcus P. Potential-pH diagrams for hydroxyl and hydrogen adsorbed on a copper surface. Electrochim Acta 2005;51:408–17.
[33] Oger L, Lafouresse M-C, Odemer G, Peguet L, Blanc C. Hydrogen diffusion and trapping in a low copper 7xxx aluminium alloy investigated by scanning Kelvin probe force microscopy. Mater Sci Eng A 2017;706:126–35.